

# A Neutral Naphthalene Diimide [2]Rotaxane

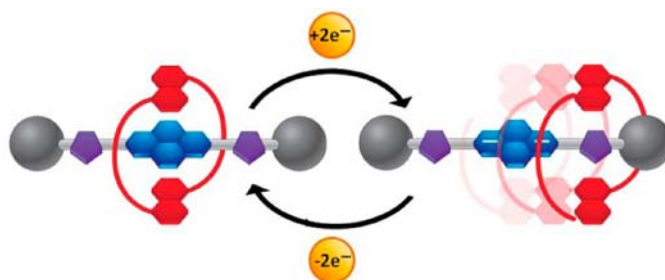
Henri-Pierre Jacquot de Rouville, Julien lehl, Carson J. Bruns, Psaras L. McGrier,  
Marco Frascioni, Amy A. Sarjeant, and J. Fraser Stoddart\*

Department of Chemistry, Northwestern University, 2145 Sheridan Road, Evanston,  
Illinois 60208-3113, United States

stoddart@northwestern.edu

Received August 17, 2012

## ABSTRACT



A neutral donor–acceptor [2]rotaxane, which has been synthesized using click chemistry, has had its solid-state structure and superstructure elucidated by X-ray crystallography. Both dynamic  $^1\text{H}$  NMR spectroscopy and electrochemical investigations have been employed in an attempt to shed light on both geometrical reorganization and redox-switching processes that are occurring or can be induced within the [2]rotaxane.

During the past 30 years, the advent of the mechanical bond<sup>1</sup> has provided a fresh incentive to chemical synthesis and opened up a whole new field of scientific research, which we have referred to as mechanostereochemistry.<sup>2</sup>

(1) (a) Frisch, H.; Martin, I.; Mark, H. *Monatsch. Chem.* **1953**, *84*, 250–256. (b) Schill, G. *Catenanes, Rotaxanes and Knots*; Academic Press: New York, 1971. (c) Amabilino, D. B.; Stoddart, J. F. *Chem. Soc. Rev.* **1995**, *95*, 2725–2828. (d) *Molecular Catenanes, Rotaxanes and Knots: A Journey through the World of Molecular Topology*; Sauvage, J.-P., Dietrich-Buchecker, C., Eds.; Wiley-VCH: Weinheim, 1999. (e) Stoddart, J. F. *Chem. Soc. Rev.* **2009**, *38*, 1521–1529 and 1802–1820. (f) Forgan, R. S.; Sauvage, J.-P.; Stoddart, J. F. *Chem. Rev.* **2011**, *111*, 5434–5464. (g) Bruns, C. J.; Stoddart, J. F. *Top. Curr. Chem.* **2012**, *323*, 19–72.

(2) Olson, M. A.; Botros, Y. Y.; Stoddart, J. F. *Pure Appl. Chem.* **2010**, *82*, 1569–1574.

(3) Deng, H.; Olson, M. A.; Stoddart, J. F.; Yaghi, O. M. *Nat. Chem.* **2010**, *2*, 439–443.

(4) (a) Cram, D. J.; Cram, J. M. *Science* **1974**, *183*, 803–809. (b) Lehn, J.-M. *Science* **1985**, *227*, 849–856. (c) Lehn, J.-M. *Angew. Chem., Int. Ed. Engl.* **1990**, *29*, 1304–1319. (d) Lehn, J.-M. *Supramolecular Chemistry: Concepts and Perspectives*; Wiley-VCH: New York, NY, 1995. (e) Rebek, J. *Chem. Soc. Rev.* **1996**, *25*, 255–264. (f) Spruell, J. M. *Pure Appl. Chem.* **2010**, *82*, 2281–2294.

(5) (a) Baxter, P.; Lehn, J.-M.; DeCian, A.; Fisher, J. *Angew. Chem., Int. Ed. Engl.* **1993**, *32*, 69–72. (b) Chichak, K. S.; Cantrill, S. J.; Pease, A. R.; Chiu, S. H.; Cave, G. W. V.; Atwood, J. L.; Stoddart, J. F. *Science* **2004**, *304*, 1308–1312. (c) Ayme, J.-F.; Beavis, J. E.; Leigh, D. A.; McBurney, R. I.; Rissanen, K.; Schultz, D. *Nat. Chem.* **2012**, *4*, 15–20. (d) Sun, Q. F.; Sato, S.; Fujita, M. *Nat. Chem.* **2012**, *4*, 330–333. (e) Belowich, M. E.; Valente, C.; Smaldone, R. A.; Friedman, D. C.; Thiel, J.; Cronin, L.; Stoddart, J. F. *J. Am. Chem. Soc.* **2012**, *134*, 5243–5261.

Countless mechanically interlocked molecules<sup>2,3</sup> (MIMs) have been synthesized by exploiting molecular recognition<sup>4</sup> and self-assembly<sup>5</sup> processes in their template-directed<sup>6</sup> synthesis. For the class of MIMs templated by aromatic donor–acceptor interactions, X-ray crystal structures of [2]catenanes<sup>7</sup> are commonplace,<sup>8</sup> whereas solid-state structures of donor–acceptor [2]rotaxanes are far more rare since they have proven to be, with a few exceptions,<sup>9</sup> much harder to crystallize on account of the flexibility of their dumbbell components.

The Sanders group has developed and popularized a family of neutral donor–acceptor catenanes<sup>10</sup> comprising

(6) (a) Busch, D. H.; Stephenson, N. A. *Coord. Chem. Rev.* **1990**, *100*, 119–154. (b) Anderson, S.; Anderson, H. L.; Sanders, J. K. M. *Acc. Chem. Rev.* **1993**, *26*, 469–475. (c) Raymo, F. M.; Stoddart, J. F. *Pure Appl. Chem.* **1996**, *68*, 313–322. (d) Breault, G. A.; Hunter, C. A.; Mayers, P. C. *Tetrahedron* **1999**, *55*, 5265–5293. (e) Griffiths, K. E.; Stoddart, J. F. *Pure Appl. Chem.* **2008**, *80*, 485–506.

(7) Not only are there a limited number of degrees of (co)-conformational freedom that the molecules of donor–acceptor [2]catenanes can adopt, but they can also, and do commonly, pack as extended donor–acceptor  $\pi$ – $\pi$  stacks at the supramolecular level in the crystal.

(8) Zhao, Y.-L.; Shveyd, A. K.; Stoddart, J. F. *Tetrahedron Lett.* **2011**, *52*, 2044–2047.

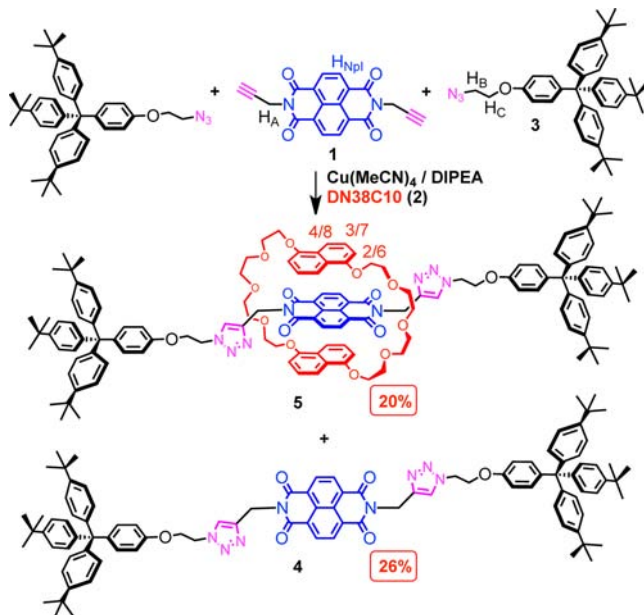
(9) (a) Yoon, I.; Miljanić, O. Š.; Benitez, D.; Khan, S. I.; Stoddart, J. F. *Chem. Commun.* **2008**, *38*, 4561–4563. (b) Slater, B. J.; Davies, E. S.; Argent, S. P.; Nowell, H.; Lewis, W.; Blake, A. J.; Champness, N. R. *Chem.—Eur. J.* **2011**, *17*, 14746–14757.

1,5-dinaphtho[38]crown-10<sup>11</sup> (DN38C10) rings interlocked with relatively rigid macrocycles containing naphthalene diimide (NpI) units,<sup>12</sup> which are prepared by Eglinton couplings of terminal acetylenes. Since Eglinton couplings fall short of the ideal of kinetic covalent chemistry<sup>13</sup> (KCC) in MIM production—an approach requiring that the coupling reaction is all but quantitative, particularly when it is employed more than once—the modification of Huisgen's 1,3-dipolar cycloaddition<sup>14</sup> between an azide and an alkyne in the context of the copper(I)-catalyzed azide–alkyne cycloaddition<sup>15</sup> (CuAAC) represents an attractive alternative. The CuAAC reaction, which embodies the kind of 'click chemistry' envisioned<sup>16</sup> by Sharpless, provides a highly efficient means<sup>17</sup> of producing rotaxanes and catenanes and has led<sup>18</sup> to the production of a wide range of MIMs in good yields from readily available starting materials.

Here, we report (i) the synthesis, employing click chemistry, of a neutral NpI-based [2]rotaxane which, following (ii) its solid-state characterization by X-ray crystallography, is investigated for (iii) its solution-state properties by <sup>1</sup>H NMR spectroscopy and electrochemical experiments.

In the synthesis (Scheme 1) of the [2]rotaxane **5**, DN38C10 (**2**) was stirred in PhMe with **1**<sup>19</sup> and an immediate change in color was observed from colorless to purple, marking the formation of the 1:1 inclusion complex **1** ⊂ **2**. After complete solubilization of **1** by **2**, 2.2 equiv of **3**<sup>19</sup> were added to the reaction mixture,<sup>20</sup> followed by a catalytic amount of Cu(MeCN)<sub>4</sub>PF<sub>6</sub> and diisopropylethylamine (DIPEA). The pure [2]rotaxane **5** and its corresponding free dumbbell **4** were isolated by column (SiO<sub>2</sub>: CH<sub>2</sub>Cl<sub>2</sub>/MeOH, 97:3) and gel permeation chromatography (Biobeads SX-1: CH<sub>2</sub>Cl<sub>2</sub>) in 20 and 26% yields, respectively.

**Scheme 1.** Synthesis of the [2]Rotaxane **5** and Its Dumbbell **4** According to a Convergent Approach Using the Huisgen 1,3-Dipolar Cycloaddition



Single crystals suitable for X-ray analysis<sup>21</sup> were obtained by slow diffusion of MeOH into a solution of **5** in C<sub>6</sub>H<sub>6</sub>. The solid-state structure (Figure 1) of **5** reveals that it has a center of symmetry. While the NpI unit in the dumbbell component of the rotaxane is encircled by the DN38C10 ring in such a manner that the 1,5-dioxy-naphthalene (DNP) units of the crown ether are  $\pi$ – $\pi$  stacking with it at the short plane-to-plane separation of 3.29 Å, the polyether loops of the DN38C10 ring are interacting through [C–H···O] close contacts of 3.33 Å for the shortest [C···O] distance. In the superstructure (see Supporting Information (SI)), the macrocycles are packed in a herringbone arrangement in a plane along the median of the *a* and *b* axes of the unit cell with the dumbbells oriented orthogonally therein, and the rotaxanes stack on top of each other with a slight offset along the *b* axis.

The <sup>1</sup>H NMR spectra (Figure 2) of both the dumbbell **4** and the [2]rotaxane **5** can best be interpreted in terms of their molecules exhibiting averaged C<sub>2v</sub> symmetry. In the case of **5**, this averaging of its molecular symmetry has to involve the rapid reorientation of the two DNP units in the DN38C10 ring at room temperature, most likely as a result of the crown ether forsaking its  $\pi$ – $\pi$  stacking interactions with the NpI unit in order to execute the necessarily rapid pedaling motions, on the <sup>1</sup>H NMR time scale, around the central C–C bonds of both DNP units. In support of the  $\pi$ – $\pi$  stacking of the NpI acceptor unit with the two DNP donor units in the [2]rotaxane, the chemical shift ( $\delta$ ) of the

(10) (a) Hamilton, D. G.; Davies, J. E.; Prodi, L.; Sanders, J. K. M. *Chem.—Eur. J.* **1998**, *4*, 608–620. (b) Cougnon, F. B. L.; Jenkins, N. A.; Pantos, D. G.; Sanders, J. K. M. *Angew. Chem., Int. Ed.* **2012**, *51*, 1443–1447.

(11) Bruns, C. J.; Basu, S.; Stoddart, J. F. *Tetrahedron Lett.* **2008**, *51*, 983–986.

(12) DN38C10 and NpI exhibit a strong association in apolar and polar aprotic solvents. See: Hamilton, D. G.; Montalti, M.; Prodi, L.; Fontani, M.; Zanello, P.; Sanders, J. K. M. *Chem.—Eur. J.* **2000**, *6*, 608–617.

(13) Ke, C.; Smaldone, R. A.; Kikuchi, T.; Li, H.; Davis, A. P.; Stoddart, J. F. *Angew. Chem., Int. Ed.* **2012**, *10.1002/anie.201205087*.

(14) (a) Huisgen, R.; Szeimies, G.; Möbius, L. *Chem. Ber.* **1967**, *100*, 2494–2507. (b) Huisgen, R. *Pure Appl. Chem.* **1989**, *61*, 613–628.

(15) (a) Rostovtsev, V. V.; Green, L. G.; Fokin, V. V.; Sharpless, K. B. *Angew. Chem., Int. Ed.* **2002**, *41*, 2596–2599. (b) Tornøe, C. W.; Christensen, C.; Meldal, M. *J. Org. Chem.* **2002**, *67*, 3057–3064.

(16) Kolb, H. C.; Finn, M. G.; Sharpless, K. B. *Angew. Chem., Int. Ed.* **2001**, *40*, 2004–2021.

(17) Aucagne, V.; Hänni, K. D.; Leigh, D. A.; Lusby, P. J.; Walker, D. B. *J. Am. Chem. Soc.* **2006**, *128*, 2186–2187. (b) Dichtel, W. R.; Miljanić, O. Š.; Health, J. R.; Stoddart, J. F. *J. Am. Chem. Soc.* **2006**, *128*, 10388–10390.

(18) (a) Hänni, K. D.; Leigh, D. A. *Chem. Soc. Rev.* **2010**, *39*, 1240–1251. (b) Fahrenbach, A. C.; Stoddart, J. F. *Chem.—Asian J.* **2011**, *6*, 2660–2669.

(19) See the Supporting Information: all compounds were characterized fully by <sup>1</sup>H and <sup>13</sup>C NMR spectroscopies and mass spectrometry. The assignments of <sup>1</sup>H and <sup>13</sup>C resonances were made as a result of 2D NMR experiments, i.e., COSY, HSQC, and HMBC.

(20) It is noteworthy that the reaction mixture had to be degassed to prevent the poisoning of the catalyst and side reactions: in the presence of O<sub>2</sub> the oxidation of Cu(I) to Cu(II) can take place, giving rise to the polymerization of **1** as a result of multiple Eglinton couplings.

(21) Crystal data for [2]rotaxane (**5**): C<sub>36</sub>H<sub>44</sub>O<sub>10</sub>, C<sub>98</sub>H<sub>104</sub>N<sub>8</sub>O<sub>6</sub>, pink plate, crystal size 0.328 × 0.293 × 0.04 mm<sup>3</sup>, monoclinic, space group, P2<sub>1</sub>/c, *a* = 22.5961(6) Å, *b* = 18.2223(5) Å, *c* = 14.5264(5) Å,  $\alpha$  = 90.00°,  $\beta$  = 96.378(2)°,  $\gamma$  = 90.00°, *V* = 5944.3(3) Å<sup>3</sup>, *Z* = 2,  $\rho_{\text{calcd}}$  = 1.188, *T* = 100(2) K, *R*<sub>1</sub>(*F*<sup>2</sup> > 2σ*F*<sup>2</sup>) = 0.1508, *wR*<sub>2</sub> = 0.4090.

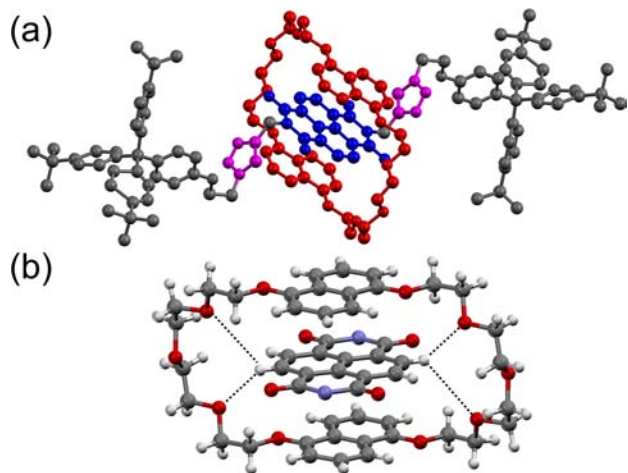


**Figure 1.** Solid state structure of the [2]rotaxane **5**. (a) Perspective drawing of the [2]rotaxane (hydrogens have been omitted for clarity). (b) The DN38C10 ring and NpI interact through  $\pi$ - $\pi$  stacking and [C-H $\cdots$ O] close contacts between the polyether loops and the NpI protons.

resonances for the NpI and triazole protons in **5** are shifted upfield by 0.48 ppm and downfield by 0.24 ppm, respectively, with respect to their  $\delta$  values in the free dumbbell **4**, while the signals for H<sub>2/6</sub>, H<sub>3/7</sub>, and H<sub>4/8</sub> in the DN38C10 ring are shifted upfield by ca. 0.5 ppm with respect to their  $\delta$  values in the free crown ether. Variable temperature <sup>1</sup>H NMR experiments were also performed in CD<sub>2</sub>Cl<sub>2</sub> in order to assess the reorientation of the DNP units in the DN38C10 ring (see SI). Upon cooling the solution down to 199 K, the singlet observed at  $\delta = 8.27$  ppm for the NpI protons at ambient temperature broadens ( $T_c = 227$  K), while also moving to higher field, and then separates out into an AB system with  $\delta_A = 8.14$  and  $\delta_B = 8.11$  ppm.

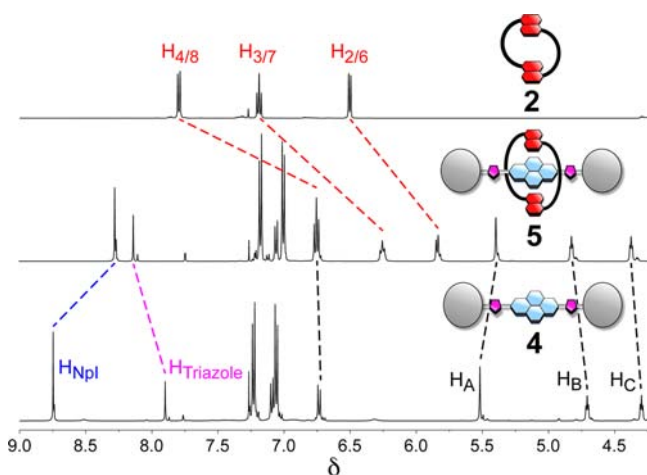


**Figure 2.** Partial <sup>1</sup>H NMR spectra (500 MHz) recorded at room temperature in CDCl<sub>3</sub> of the DN38C10 ring **2** (top), the rotaxane **5** (middle), and the corresponding dumbbell **4** (bottom).

An approximate calculation reveals that this temperature dependent behavior, which is associated with a free energy barrier of 11.3 kcal mol<sup>-1</sup>, can be attributed to the slowing down, on the <sup>1</sup>H NMR time scale, of the degenerate reorganization of the DNP rings in DN38C10 such that they impose their local C<sub>2</sub> symmetry on the NpI units.

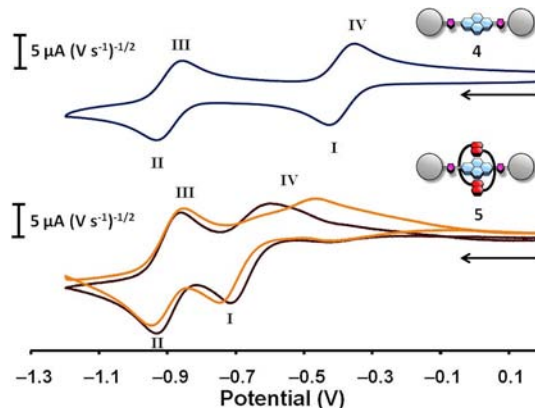


**Figure 3.** Cyclic voltammograms of the dumbbell **4** (top) at a scan rate of 100 mV·s<sup>-1</sup> and rotaxane **5** (bottom) at scan rates of 50 mV·s<sup>-1</sup> in dark red and 500 mV·s<sup>-1</sup> in orange ( $c = 1 \times 10^{-3}$  mol·L<sup>-1</sup> in DMF with 0.1 mol·L<sup>-1</sup> of TBAPF<sub>6</sub>). All scans have been normalized to the square root of the scan rate.

Electrochemical experiments, namely, cyclic voltammetry (CV) and differential pulse voltammetry (DPV), were performed at 298 K in Ar-purged DMF and CH<sub>2</sub>Cl<sub>2</sub> solutions with 0.1 mol·L<sup>-1</sup> TBAPF<sub>6</sub> as the supporting electrolyte. All potentials are referenced against a Ag/AgCl electrode (SSCE). A comparison between the CV (Figure 3) of the free dumbbell **4** and that of the [2]rotaxane **5** in DMF allows for elucidation of the electrochemically induced shuttling mechanism.<sup>22</sup> At 50 mV·s<sup>-1</sup> in DMF, the first reduction (I, NpI → NpI<sup>•-</sup>) of **5** is dramatically shifted to higher potential (ca. -0.70 V) compared to the first reduction wave of **4** at -0.39 V. This shift can be explained by the interaction between the DN38C10 ring and the NpI unit, since the electron density transferred from the DNP donors makes it more difficult to reduce NpI. On the contrary, compounds **4** and **5** share virtually identical second reduction waves (II, NpI<sup>•-</sup> → NpI<sup>2-</sup>) near -0.90 V, suggesting that the ring moves away from its station after reduction and does not associate with the radical anion NpI<sup>•-</sup>. Likewise, the first reoxidation step (III, NpI<sup>2-</sup> → NpI<sup>•-</sup>) is essentially identical for the dumbbell and the rotaxane on account of the ring having no association with NpI<sup>2-</sup>. The final reoxidation (IV, NpI<sup>•-</sup> → NpI) to regenerate the neutral species occurs at a lower potential than would be expected for a reversible process. The irreversibility of this redox process at I and IV is not unexpected, since the ring resides around NpI at I but is absent at IV, meaning the rotaxane does not

(22) Several scans were performed on the same sample of **5** in order to confirm that the voltammograms remain unchanged, establishing the stability of the [2]rotaxane and the repeatability of the redox process.



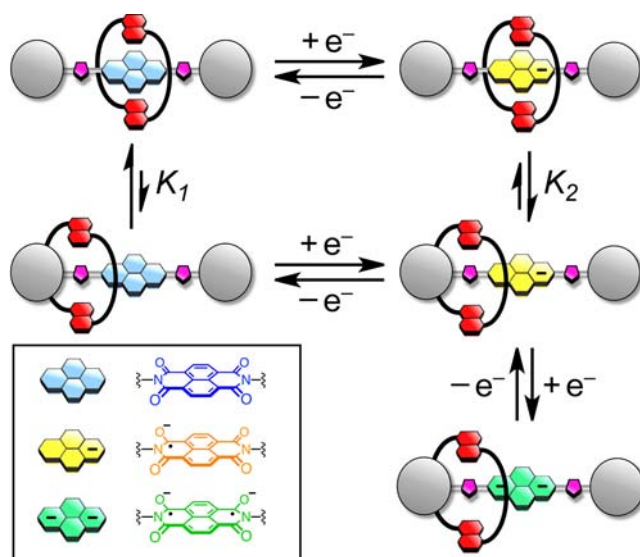
return to the ground state by the same path it followed at the outset.

Variable scan-rate CV of **5** revealed that only process **IV** is scan-rate dependent in DMF, where the oxidation potential shifts closer to that of the free dumbbell at  $500 \text{ mV}\cdot\text{s}^{-1}$ . This phenomenon could be interpreted as a result of the ring passing over the  $\text{NpI}^{\bullet-}$  station as it shuttles back and forth along the entire dumbbell, with less likelihood of ‘catching’ the ring on the  $\text{NpI}^{\bullet-}$  station at fast scan rates. By contrast, translational motion has enough time to equilibrate between data points at a slow scan rate, making the redox process appear more reversible. Similar redox behavior was observed in  $\text{CH}_2\text{Cl}_2$ . See Figure S3a–c in the SI. Although the irreversibility of the CV precludes an accurate calculation<sup>23</sup> of the equilibrium constant  $K_1$  governing the ground state distribution of translational isomers, we can estimate a lower limit  $K_1 > 10000 \text{ M}^{-1}$  in DMF based on the magnitude of the dramatic shift of **I** and **IV** in rotaxane **5** with respect to dumbbell **4**, indicating that the ring’s association with the triazole units is extremely small. Thus, the rotaxane can be described as a ‘push button’<sup>24</sup> with two states (on/off) since no metastable translational isomer persists for a significant period of time following redox-stimulated switching events.

Both **4** and **5** were investigated (see SI) by spectroelectrochemistry (SEC) in  $\text{CH}_2\text{Cl}_2$  at  $1 \text{ mmol}\cdot\text{L}^{-1}$ . The optical spectrum of **5** shows a characteristic absorption band at 500 nm arising from a charge-transfer (CT) interaction between the  $\text{NpI}$  and DNP units in the DN38C10 ring. This observation agrees with the reported wavelength in the literature<sup>25</sup> and supports the claim that the ring resides primarily on the  $\text{NpI}$  unit in the neutral form. At an applied potential of  $-1.2 \text{ V}$ , the reduced species **4**<sup>2-</sup> and **5**<sup>2-</sup> are generated, giving rise to similar spectra with two bands at 680 and 750 nm that are attributed to the diradical dianion  $\text{NpI}^{2-}$ , accompanied by a disappearance of the CT absorption band in the case of **5**. Following reoxidation at a potential of 0.0 V, the original spectra of the neutral compounds are restored, indicating that no significant decomposition occurs during the reduction cycle.

The proposed shuttling mechanism of the [2]rotaxane **5**, which is based on the CV and SEC experiments, is depicted in Scheme 2. In the neutral form, the ring shuttles between

**Scheme 2.** Proposed Mechanism for the Electrochemically Induced Shuttling of the [2]Rotaxane **5**



$\text{NpI}$  and either one of the triazole units, with the vast majority of its time spent around the  $\text{NpI}$  unit. On the contrary, when  $\text{NpI}$  is reduced to  $\text{NpI}^{\bullet-}$ , the ring shuttles along the length of the dumbbell with little association for any site in particular.

In summary, we have described the synthesis, solid-state structure, and electrochemically driven ‘push-button’ switching mechanism of the neutral [2]rotaxane **5**. The neutral, rigid structure of the rotaxane renders it a suitable candidate for high resolution imaging by scanning tunneling microscopy in future studies.

**Acknowledgment.** We acknowledge support from the Non-Equilibrium Energy Research Center (NERC), which is an Energy Frontier Research Center (EFRC) funded by the U.S. Department of Energy, Office of Basic Sciences (DOE-BES) under Award DE-SC0000989. J.F.S. and C.J.B. were supported by the WCU Program (NRF R-31-2008-000-10055-0) funded by the Ministry of Education, Science and Technology, Korea. C.J.B. acknowledges support from an NSF Graduate Research Fellowship. P.L.M. acknowledges the NSF and Georgia Tech Facilitating Academic Careers in Engineering and Science (FACES) committee for a postdoctoral fellowship.

**Supporting Information Available.** Experimental details. This material is available free of charge via the Internet at <http://pubs.acs.org>.

The authors declare no competing financial interest.

(23) For a detailed discussion of our approach to estimating ground state distributions in MIMs by CV, see: (a) Fahrenbach, A. C.; Barnes, J. C.; Li, H.; Benítez, D.; Basuray, A. N.; Fang, L.; Sue, C.-H.; Barin, G.; Dey, S. K.; Goddard, W. A., III; Stoddart, J. F. *Proc. Natl. Acad. Sci. U.S.A.* **2011**, *108*, 20416–20421. (b) Fahrenbach, A. C.; Bruns, C. J.; Cao, D.; Stoddart, J. F. *Acc. Chem. Res.* **2012**, *45*, 1581–1592.

(24) Spruell, J. M.; Paxton, W. F.; Olsen, J.-C.; Benítez, D.; Tkatchouk, E.; Stern, C. L.; Trabolsi, A.; Friedman, D. C.; Goddard, W. A., III; Stoddart, J. F. *J. Am. Chem. Soc.* **2009**, *131*, 11571–11580.

(25) Dey, S. K.; Coskun, A.; Fahrenbach, A. C.; Barin, G.; Basuray, A. N.; Trabolsi, A.; Botros, Y. Y.; Stoddart, J. F. *Chem. Sci.* **2011**, *2*, 1046–1053.